RESEARCH ARTICLE

Check for updates

An indium-based microporous metal–organic framework with unique three-way rod-shaped secondary building units for efficient methane and hydrogen storage†

Hui Cui,‡[a,b] Yingxiang Ye, [iD] ‡[c] Ruibiao Lin, [iD] [d] Yanshu Shi,[a] Zeid A. Alothman, [iD] [e] Osamah Alduhaish,[e] Bin Wang, [iD] *[c] Jian Zhang[f] and Banglin Chen [iD] *[a]

A novel microporous indium-based MOF material with unique 3-way rod-shaped secondary building units (SBUs), UTSA-22, was reported and exhibited high methane (CH_4) and hydrogen (H_2) storage. At 298 K and 65 bar, the total CH_4 volumetric uptake of UTSA-22 is 174 cm^3(STP) cm^{-3}. Moreover, UTSA-22 shows a high CH_4 working capacity of 146 cm^3(STP) cm^{-3} in a pressure range of 5–65 bar at 298 K. In addition, UTSA-22 shows a high H_2 gravimetric storage capacity (1.2 wt%) at 298 K and 100 bar.

As a primary greenhouse gas, carbon dioxide has been released globally to reach a record high level as fossil fuel demand is growing tremendously. Methane (CH_4), a primary component in natural gas, is considered a potential alternative to liquid fossil fuels since it is clean, abundant, and renewable on earth.[1] However, low energy densities have limited its practical applications. In this regard, to utilize methane as a transportation fuel, a suitable adsorbent with high CH_4 storage capacity at low pressures will be required (when methane is used as a transportation fuel stored by an adsorbent).[2] Therefore, significant interest has been shown in adsorbed natural gas systems to overcome these problems, including filling the tank with porous materials for storing high-density methane at moderate pressures. According to the guidelines of the department of energy (DOE) in the U.S.,[3] ambitious targets for volumetric and gravimetric capacities for CH_4 storage are up to 350 cm^3(STP) cm^{-3} and 0.5 g/g, respectively, at room temperature (R.T.) for the next generation of clean energy auto-mobiles when considering the ignored loss of the packing adsorbent. Thus, comprehensive research efforts are being devoted to developing novel adsorbent materials with high CH_4 storage capacity to achieve these challenging storage goals.[4,5]

Owing to their high Brunauer–Emmett–Teller (BET) surface areas and tunable pore functions, metal–organic frameworks (MOFs) are emerging as a new generation of crystalline materials that are able to outperform conventionally used activated carbon, zeolites, and silica gels in a multitude of different physico-chemical aspects.[6–15] Large numbers of MOFs have been demonstrated to be promising for CH_4 storage, considering both volumetric and gravimetric CH_4 uptake and storage.[16–24] It is worth noting that the CH_4 volumetric working capacity (also known as deliverable capacity) is considered to be a much more important parameter to assess the performance of these absorptive materials for practical applications due to the limitations of gas tanks in vehicles, which reflects the actual driving range using natural gas.[25–27] At present, to achieve a high working capacity, it is necessary to maximize the amount of methane stored at high pressure and minimize methane storage at low pressure (around 5 bar).[28–30] Several strategies have been proven to improve the CH_4 working capacity, such as optimizing pore structure, tuning the framework's flexibility, and incorporating strong binding sites.[31–35] However, it is still challenging to optimize the pore structure with an appropriate CH_4 binding affinity for balancing the trade-off of methane adsorption between low and high pressures to therefore obtain a superior volumetric working capacity.[36–39]

Herein, a three-dimensional microporous metal–organic framework $[In_5(TTETA)_{11/3}(OH)_4(H_2O)\cdot30H_2O\cdot19DMF]$

[a]*Department of Chemistry, University of Texas at San Antonio, One UTSA Circle, San Antonio, Texas, 78249-0698 USA*

[b]*Physics Division, Argonne National Laboratory, Lemont, IL 60439, USA*

[c]*Department of Chemistry, University of North Texas, Denton, TX 76201, USA*

[d]*MOE Key Laboratory of Bioinorganic and Synthetic Chemistry, School of Chemistry, Sun Yat-Sen University, Guangzhou, 510006 P. R. China*

[e]*Chemistry Department, College of Science, King Saud University, Riyadh 11451, Saudi Arabia*

[f]*Molecular Foundry, Lawrence Berkeley National Laboratory, Berkeley, California 94720, USA*

†Electronic supplementary information (ESI) available. CCDC 2204487. For ESI and crystallographic data in CIF or other electronic format see DOI: https://doi.org/10.1039/d2qi01956f

‡These authors contributed equally to this work.

This journal is © the Partner Organisations 2022

Inorg. Chem. Front., 2022, **9**, 6527–6533 | **6527**

(**UTSA-22**, H₃TTETA = 4,4′,4″-((2,4,6-trimethylbenzene-1,3,5-triyl)tris(ethyne-2,1-diyl)) tribenzoic acid), with unique 3-way rod-shaped SBUs, was synthesized under solvothermal conditions. It was found that the activated **UTSA-22** shows a high methane uptake of 174 cm³(STP) cm⁻³ at 298 K and 65 bar, which is higher than those of DUT-4 (164 cm³(STP) cm⁻³),[3] Fe-NDC (160 cm³(STP) cm⁻³)[40] and VNU-22 (155 cm³(STP) cm⁻³).[40] Moreover, this uptake value is comparable to some of the top performing materials when considering the significantly low surface area of **UTSA-22** (2173 m² g⁻¹), such as MOF-205 (183 cm³(STP) cm⁻³),[41] FJI-H23 (179 cm³(STP) cm⁻³),[42] and BUT-22 (182 cm³(STP) cm⁻³).[16] Additionally, the H₂ storage capacity of **UTSA-22** can reach 1.2 wt% (8.45 g L⁻¹) at 100 bar and 298 K.

Solvothermal reactions of H₃TTETA with In(NO₃)₃·6H₂O and nitric acid yielded single crystals of **UTSA-22**. Single-crystal X-ray diffraction analysis revealed that **UTSA-22** crystallizes in the trigonal system, space group $R\bar{3}c$. Three independent In³⁺ atoms, 11/6 TTETA³⁻ ligands, and one μ₂-OH⁻ group were observed in the asymmetric unit of **UTSA-22**. Both In³⁺ atoms are coordinated with four carboxylate O atoms coming from four different TTETA³⁻ ligands in the equatorial positions and two μ₂-OH⁻ groups in the apical positions. The lengths of In–O and In–OH bonds are in the ranges of 2.050(4)–2.209(6) and 2.026(6)–2.094(6) Å, respectively (Table S2†). For the TTETA³⁻ ligand, two carboxyl groups coordinate with two adjacent In³⁺ atoms in a bi-monodentate coordination, and the remaining carboxyl group coordinates with the In³⁺ atom in a monodentate mode (Fig. 1). The uncoordinated carboxylate O atom (O12) can form hydrogen bonding interactions with a μ₂-OH⁻ group (O2, the distance is 2.6 Å, Fig. S1†). The connection of In³⁺ atoms with carboxylate and μ₂-OH⁻ groups in the order of "In1–In2–In3–In2–In1" results in infinite rod-shaped secondary building units (SBUs). The SBUs are bridged by TTETA³⁻ ligands making a three-dimensional structure with one type of double-wall disordered octahedral cage (Fig. S2†). The diameter of the octahedral cage is about 18 Å. In addition, two types of pore walls with thicknesses of 3.6 and 7.7 Å, respectively, are observed in **UTSA-22** (Fig. S3†). Interestingly, the 1D chains in **UTSA-22** are arranged in a three-way model, which differs from the commonly observed one-way or two-way models (Fig. 1).[43–46] Similar SBUs have been reported in a recently published work.[47] It should be pointed out that, while preparing this manuscript, the single crystal structure of **UTSA-22** was reported by Li and co-workers, and this MOF was used for the detection of selective antibiotics in water.[48] The total potential solvent accessible void volume of the framework is 65% of the whole structure as estimated by PLATON.[49]

The phase purity of **UTSA-22** was examined by powder X-ray diffraction (PXRD) measurements (Fig. S5†). The PXRD peaks of the as-synthesized sample match with those of simulated ones obtained from the single-crystal data, proving the high phase purity of **UTSA-22**. The crystal structure remains intact after activation. In the thermogravimetric analysis (TGA) curve, two steps of weight loss were clearly observed: one is in the temperature range of 21–69 °C with a weight loss of 12%, and the other one is in the temperature range of 69–137 °C with a weight loss of 30% (Fig. S6†). By considering that in the synthesis of **UTSA-22**, only water, DMF, and HNO₃ (10 μL, 16 M) are used, and the trace HNO₃ will decompose to NO₂ at high temperature, it is thus believed that the two steps of weight loss belong to that of water and DMF in the pores of **UTSA-22**, respectively. The calculated amount of water and DMF molecules in the pores of **UTSA-22** are 30 and 19, respectively,
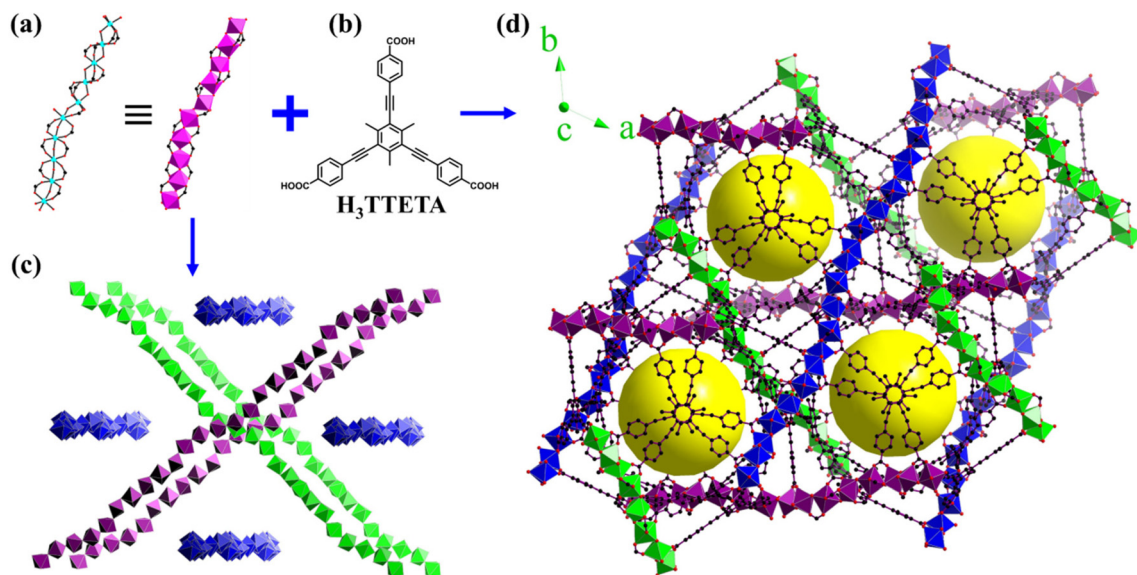

Fig. 1 (a) Infinite 1D rod-shaped SBUs, (b) structural formula of the ligand, H₃TTETA, (c) the packing of the SBUs, and (d) a three-dimensional framework structure of **UTSA-22** viewed along the crystallographic *c*-axis (color code: In, turquoise; C, black; and O, red; an octahedral geometry constituted by In and O; and hydrogen atoms are omitted for clarity).

6528 | *Inorg. Chem. Front.*, 2022, **9**, 6527–6533

This journal is © the Partner Organisations 2022

which is reasonable considering the large cell parameters ($a = b = 51.504(3)$ Å, $c = 50.096(4)$ Å; $\alpha = \beta = 90°$, $\gamma = 120°$; and $v = 115\,083(17)$ Å^3) of the host framework. The framework of **UTSA-22** is stable up to ~400 °C, followed by its decomposition (Fig. S6†). Besides, in the FT-IR spectra, a slight red shift of the characteristic peaks belonging to the carbonyl group in **UTSA-22** was observed compared with those of the H_3TTETA ligand, demonstrating the coordination between the carboxylate groups and metals (Fig. S7†). At 77 K, **UTSA-22** was examined by N_2 adsorption to achieve permanent porosity (Fig. 2a). The saturated N_2 uptake of **UTSA-22** is 581 cm^3(STP) g^{-1}, corresponding to 2173 m^2 g^{-1} as the BET surface area (Fig. S8 and S9†). Therefore, the experimental total pore volume of **UTSA-22** is 0.90 cm^3 g^{-1}, which is close to the theoretical value of 0.93 cm^3 g^{-1} by PLATON calculation.

The CH_4 storage capacity of **UTSA-22** was explored from the beginning accordingly. At 273 and 298 K, CH_4 adsorption isotherms were measured from 0 to 80 bar, respectively. As shown in Fig. 2b, at 35 bar and 298 K, the total gravimetric CH_4 uptake of **UTSA-22** is 183 cm^3(STP) g^{-1}, exceeding the DOE's previous goal (180 cm^3(STP) g^{-1}), without regard for packing density loss. At 65 and 80 bar, the total gravimetric CH_4 uptake rates of **UTSA-22** are 249 and 268 cm^3(STP) g^{-1} at 298 K, which correspond to 0.179 and 0.192 g/g, respectively, which are much higher than those of some benchmark MOFs such as Ni-MOF-74 (210 (223) cm^3(STP) g^{-1}),[50] VNU-22 (132 (140) cm^3(STP) g^{-1}),[40] and Cu-tbo-MOF-5 (208 (225) cm^3(STP) g^{-1})[50] under identical conditions (Table S3†). In addition, at 80 bar and 298 K, the volumetric CH_4 uptake is 188 cm^3(STP) cm^{-3}, comparable to those of VNU-21 (194 cm^3(STP) cm^{-3}),[40]
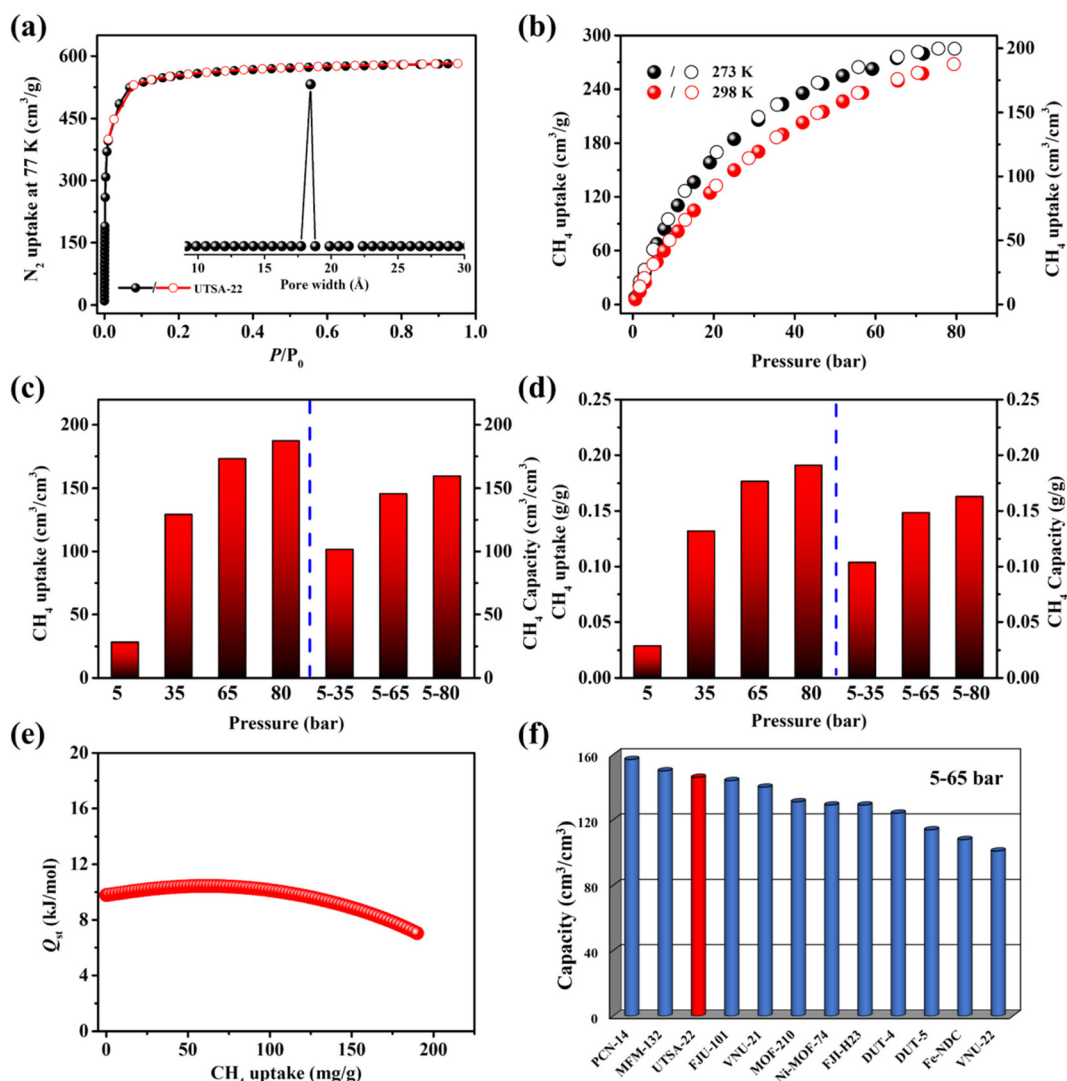

Fig. 2 (a) N_2 adsorption/desorption isotherms for **UTSA-22** at 77K; (b) CH_4 isotherms at 273 and 298 K for **UTSA-22** up to 80 bar. Solid symbols: adsorption and open symbols: desorption. (c) Volumetric and (d) gravimetric CH_4 uptake (at 5, 35, 65, and 80 bar, respectively)/working capacities (in the pressure ranges of 35−5, 65−5, and 80−5 bar, respectively) of **UTSA-22** at 298 K. (e) Q_{st} of CH_4 for **UTSA-22** obtained using the virial method; and (f) comparison of the volumetric CH_4 working capacities (5−65 bar) of **UTSA-22** with some benchmark MOF materials.

BUT-22 (202 cm^3(STP) cm^{-3}),[16] and MFM-132 (213 cm^3(STP) cm^{-3}).[34]

The working capacity is another important factor that needs to be considered while assessing porous materials for practical methane storage. The working capacity is the difference in the total adsorption from 5 to 80 (or 65) bar. As shown in Table S3,† at 298 K, the CH_4 volumetric working capacity (65–5 bar) for **UTSA-22** is 146 cm^3(STP) cm^{-3}, which is comparable or higher than those widely explored MOFs like Ni-MOF-74 (129 cm^3(STP) cm^{-3}),[50] FJU-101 (144 cm^3(STP) cm^{-3}),[17] DUT-4 (124 cm^3(STP) cm^{-3}),[3] and VNU-22 (101 cm^3(STP) cm^{-3}).[40] When the temperature is reduced to 273 K, the CH_4 volumetric working capacity (65–5 bar) increases to 157 cm^3(STP) cm^{-3}, which is higher than some well-known microporous MOFs such as NiMOF-74 (106 cm^3(STP) cm^{-3}),[51] ZJU-70 (134 cm^3(STP) cm^{-3}),[52] MOF-505 (112 cm^3(STP) cm^{-3}),[53] and PCN-14 (153 cm^3(STP) cm^{-3}).[51] Additionally, the adsorption enthalpy (Q_{st}) of **UTSA-22** is 9.8 kJ mol^{-1} (Fig. 2e), which is lower than that found for most reported MOFs (Table S3†). Such a low adsorption enthalpy involving host–guest interactions is significantly important when CH_4 gas is released from the gas tank.

The H_2 isotherms of **UTSA-22** were recorded up to 100 bar at 273 and 298 K. As shown in Fig. 3, the gravimetric H_2 of **UTSA-22** at 298 K and 100 bar is 1.2 wt%, which is higher than the values for most reported MOFs, such as $Co_2(BDC)_2$(dabco) (0.32 wt%),[54] $Cu_2(BDC)_2$(dabco) (0.42 wt%),[54] JUC-48 (1.1 wt%),[55] Mg_2(dobdc) (0.8 wt%),[56] and Cu(peip) (0.46 wt%)[57] under identical conditions. Besides, **UTSA-22** shows a remarkably high H_2 volumetric uptake of 8.45 g L^{-1} at 298 K and 100 bar, which is higher than some famous MOFs such as NU-1501-Al (8.40 g L^{-1})[58] and Mg_2(dobdc) (7.50 g L^{-1}).[56] The Q_{st} of H_2 for **UTSA-22** is 12.3 kJ mol^{-1} at zero bar based on the isotherms obtained at 298 and 273 K (Fig. S12†).
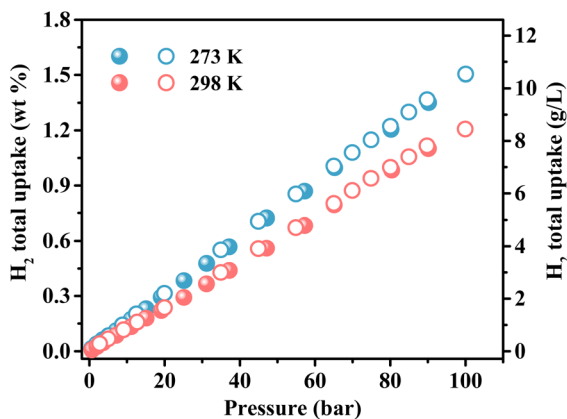

Fig. 3 High-pressure hydrogen adsorption isotherms for **UTSA-22** at 273 and 298 K.

Conclusions

A novel microporous In-based MOF with unique three-way rod-shaped SBUs, named **UTSA-22**, has been designed and synthesized for efficient CH_4 and H_2 storage. Owing to its cage-type structure, **UTSA-22** has a modest BET surface area of 2173 m^2 g^{-1} and is stable up to 400 °C. **UTSA-22** shows a high CH_4 gravimetric storage capacity of 268 cm^3(STP) g^{-1} (0.192 g/g) at 80 bar and 298 K. The CH_4 volumetric delivery capacity (65–5 bar) of **UTSA-22** is 146 cm^3(STP) cm^{-3} at 298 K, comparable to or higher than some benchmark MOF materials. Furthermore, the H_2 gravimetric uptake is 1.2 wt% for **UTSA-22** at 298 K and 100 bar. Therefore **UTSA-22** can be potentially used in CH_4 and H_2 storage applications.

Conflicts of interest

There are no conflicts to declare.

Acknowledgements

References

1 J. Jiang, H. Furukawa, Y.-B. Zhang and O. M. Yaghi, High Methane Storage Working Capacity in Metal–Organic Frameworks with Acrylate Links, *J. Am. Chem. Soc.*, 2016, **138**, 10244–10251.

2 T. A. Makal, J.-R. Li, W. Lu and H.-C. Zhou, Methane storage in advanced porous materials, *Chem. Soc. Rev.*, 2012, **41**, 7761–7779.

3 Y. He, W. Zhou, G. Qian and B. Chen, Methane storage in metal–organic frameworks, *Chem. Soc. Rev.*, 2014, **43**, 5657–5678.

4 Z. Chen, M. R. Mian, S.-J. Lee, H. Chen, X. Zhang, K. O. Kirlikovali, S. Shulda, P. Melix, A. S. Rosen, P. A. Parilla, T. Gennett, R. Q. Snurr, T. Islamoglu, T. Yildirim and O. K. Farha, Fine-Tuning a Robust Metal–Organic Framework toward Enhanced Clean Energy Gas Storage, *J. Am. Chem. Soc.*, 2021, **143**, 18838–18843.

5 J. A. Mason, J. Oktawiec, M. K. Taylor, M. R. Hudson, J. Rodriguez, J. E. Bachman, M. I. Gonzalez, A. Cervellino,

6530 | *Inorg. Chem. Front.*, 2022, **9**, 6527–6533

This journal is © the Partner Organisations 2022

A. Guagliardi, C. M. Brown, P. L. Llewellyn, N. Masciocchi and J. R. Long, Methane storage in flexible metal–organic frameworks with intrinsic thermal management, *Nature*, 2015, **527**, 357–361.

6 H. Cui, Y. Ye, T. Liu, Z. A. Alothman, O. Alduhaish, R.-B. Lin and B. Chen, Isoreticular Microporous Metal–Organic Frameworks for Carbon Dioxide Capture, *Inorg. Chem.*, 2020, **59**, 17143–17148.

7 H. Cui, Y. Xie, Y. Ye, Y. Shi, B. Liang and B. Chen, An Ultramicroporous Metal-Organic Framework with Record High Selectivity for Inverse CO_2/C_2H_2 Separation, *Bull. Chem. Soc. Jpn.*, 2021, **94**, 2698–2701.

8 H. Cui, Y. Ye, H. Arman, Z. Li, A. Alsalme, R.-B. Lin and B. Chen, Microporous Copper Isophthalate Framework of mot Topology for C_2H_2/CO_2 Separation, *Cryst. Growth Des.*, 2019, **19**, 5829–5835.

9 X. Zhang, R.-B. Lin, J. Wang, B. Wang, B. Liang, T. Yildirim, J. Zhang, W. Zhou and B. Chen, Optimization of the Pore Structures of MOFs for Record High Hydrogen Volumetric Working Capacity, *Adv. Mater.*, 2020, **32**, 1907995.

10 R.-B. Lin, S. Xiang, B. Li, Y. Cui, G. Qian, W. Zhou and B. Chen, Our journey of developing multifunctional metal-organic frameworks, *Coord. Chem. Rev.*, 2019, **384**, 21–36.

11 W. Gong, H. Cui, Y. Xie, Y. Li, X. Tang, Y. Liu, Y. Cui and B. Chen, Efficient C_2H_2/CO_2 Separation in Ultramicroporous Metal–Organic Frameworks with Record C_2H_2 Storage Density, *J. Am. Chem. Soc.*, 2021, **143**, 14869–14876.

12 Y. Xie, Y. Shi, H. Cui, R.-B. Lin and B. Chen, Efficient Separation of Propylene from Propane in an Ultramicroporous Cyanide-Based Compound with Open Metal Sites, *Small Struct.*, 2022, **3**, 2100125.

13 Y. Shi, Y. Xie, H. Cui, Z. A. Alothman, O. Alduhaish, R.-B. Lin and B. Chen, An ultramicroporous metal–organic framework with dual functionalities for high sieving separation of CO_2 from CH_4 and N_2, *Chem. Eng. J.*, 2022, **446**, 137101.

14 D. Zhao, X. Wang, L. Yue, Y. He and B. Chen, Porous metal–organic frameworks for hydrogen storage, *Chem. Commun.*, 2022, **58**, 11059–11078.

15 D. Zhao, K. Yu, X. Han, Y. He and B. Chen, Recent progress on porous MOFs for process-efficient hydrocarbon separation, luminescent sensing, and information encryption, *Chem. Commun.*, 2022, **58**, 747–770.

16 B. Wang, X. Zhang, H. Huang, Z. Zhang, T. Yildirim, W. Zhou, S. Xiang and B. Chen, A microporous aluminum-based metal-organic framework for high methane, hydrogen, and carbon dioxide storage, *Nano Res.*, 2021, **14**, 507–511.

17 Y. Ye, R.-B. Lin, H. Cui, A. Alsalme, W. Zhou, T. Yildirim, Z. Zhang, S. Xiang and B. Chen, A microporous metal–organic framework with naphthalene diimide groups for high methane storage, *Dalton Trans.*, 2020, **49**, 3658–3661.

18 H.-X. Li, Z.-H. Zhang, H. Fang, D.-X. Xue and J. Bai, Synthesis, structure and high methane storage of pure D6R

Yb(Y) nonanuclear cluster-based zeolite-like metal–organic frameworks, *J. Mater. Chem. A*, 2022, **10**, 14795–14798.

19 D. Alezi, Y. Belmabkhout, M. Suyetin, P. M. Bhatt, Ł. J. Weseliński, V. Solovyeva, K. Adil, I. Spanopoulos, P. N. Trikalitis, A.-H. Emwas and M. Eddaoudi, MOF Crystal Chemistry Paving the Way to Gas Storage Needs: Aluminum-Based soc-MOF for CH_4, O_2, and CO_2 Storage, *J. Am. Chem. Soc.*, 2015, **137**, 13308–13318.

20 C. Song, Y. Ling, Y. Feng, W. Zhou, T. Yildirim and Y. He, A NbO-type metal–organic framework exhibiting high deliverable capacity for methane storage, *Chem. Commun.*, 2015, **51**, 8508–8511.

21 Q.-Y. Yang, P. Lama, S. Sen, M. Lusi, K.-J. Chen, W.-Y. Gao, M. Shivanna, T. Pham, N. Hosono, S. Kusaka, J. J. Perry IV, S. Ma, B. Space, L. J. Barbour, S. Kitagawa and M. J. Zaworotko, Reversible Switching between Highly Porous and Nonporous Phases of an Interpenetrated Diamondoid Coordination Network That Exhibits Gate-Opening at Methane Storage Pressures, *Angew. Chem., Int. Ed.*, 2018, **57**, 5684–5689.

22 T. Kundu, B. B. Shah, L. Bolinois and D. Zhao, Functionalization-Induced Breathing Control in Metal–Organic Frameworks for Methane Storage with High Deliverable Capacity, *Chem. Mater.*, 2019, **31**, 2842–2847.

23 Y. Yan, M. Juríček, F.-X. Coudert, N. A. Vermeulen, S. Grunder, A. Dailly, W. Lewis, A. J. Blake, J. F. Stoddart and M. Schröder, Non-Interpenetrated Metal–Organic Frameworks Based on Copper(II) Paddlewheel and Oligoparaxylene-Isophthalate Linkers: Synthesis, Structure, and Gas Adsorption, *J. Am. Chem. Soc.*, 2016, **138**, 3371–3381.

24 C.-C. Liang, Z.-L. Shi, C.-T. He, J. Tan, H.-D. Zhou, H.-L. Zhou, Y. Lee and Y.-B. Zhang, Engineering of Pore Geometry for Ultrahigh Capacity Methane Storage in Mesoporous Metal–Organic Frameworks, *J. Am. Chem. Soc.*, 2017, **139**, 13300–13303.

25 K. A. Forrest, G. Verma, Y. Ye, J. Ren, S. Ma, T. Pham and B. Space, Methane storage in flexible and dynamical metal–organic frameworks, *Chem. Phys. Rev.*, 2022, **3**, 021308.

26 Y. Fang, S. Banerjee, E. A. Joseph, G. S. Day, M. Bosch, J. Li, Q. Wang, H. Drake, O. K. Ozdemir, J. M. Ornstein, Y. Wang, T.-B. Lu and H.-C. Zhou, Incorporating Heavy Alkanes in Metal–Organic Frameworks for Optimizing Adsorbed Natural Gas Capacity, *Chem. – Eur. J.*, 2018, **24**, 16977–16982.

27 W. Zhou, H. Wu, M. R. Hartman and T. Yildirim, Hydrogen and Methane Adsorption in Metal−Organic Frameworks: A High-Pressure Volumetric Study, *J. Phys. Chem. C*, 2007, **111**, 16131–16137.

28 H. Li, L. Li, R.-B. Lin, W. Zhou, Z. Zhang, S. Xiang and B. Chen, Porous metal-organic frameworks for gas storage and separation: Status and challenges, *EnergyChem*, 2019, **1**, 100006.

29 C.-X. Chen, Z.-W. Wei, J.-J. Jiang, S.-P. Zheng, H.-P. Wang, Q.-F. Qiu, C.-C. Cao, D. Fenske and C.-Y. Su, Dynamic Spacer Installation for Multirole Metal–Organic

This journal is © the Partner Organisations 2022

Inorg. Chem. Front., 2022, **9**, 6527–6533 | **6531**

Frameworks: A New Direction toward Multifunctional MOFs Achieving Ultrahigh Methane Storage Working Capacity, *J. Am. Chem. Soc.*, 2017, **139**, 6034–6037.

30 T. Kundu, M. Wahiduzzaman, B. B. Shah, G. Maurin and D. Zhao, Solvent-Induced Control over Breathing Behavior in Flexible Metal–Organic Frameworks for Natural-Gas Delivery, *Angew. Chem., Int. Ed.*, 2019, **58**, 8073–8077.

31 H.-M. Wen, K. Shao, W. Zhou, B. Li and B. Chen, A novel expanded metal–organic framework for balancing volumetric and gravimetric methane storage working capacities, *Chem. Commun.*, 2020, **56**, 13117–13120.

32 M. Zhang, C. Chen, Z. Shi, K. Huang, W. Fu and W. Zhou, Inserting Amide into NOTT-101 to Sharply Enhance Volumetric and Gravimetric Methane Storage Working Capacity, *Inorg. Chem.*, 2019, **58**, 13782–13787.

33 J.-M. Lin, C.-T. He, Y. Liu, P.-Q. Liao, D.-D. Zhou, J.-P. Zhang and X.-M. Chen, A Metal–Organic Framework with a Pore Size/Shape Suitable for Strong Binding and Close Packing of Methane, *Angew. Chem., Int. Ed.*, 2016, **55**, 4674–4678.

34 Y. Yan, D. I. Kolokolov, I. da Silva, A. G. Stepanov, A. J. Blake, A. Dailly, P. Manuel, C. C. Tang, S. Yang and M. Schröder, Porous Metal–Organic Polyhedral Frameworks with Optimal Molecular Dynamics and Pore Geometry for Methane Storage, *J. Am. Chem. Soc.*, 2017, **139**, 13349–13360.

35 M. Zhang, W. Zhou, T. Pham, K. A. Forrest, W. Liu, Y. He, H. Wu, T. Yildirim, B. Chen, B. Space, Y. Pan, M. J. Zaworotko and J. Bai, Fine Tuning of MOF-505 Analogues To Reduce Low-Pressure Methane Uptake and Enhance Methane Working Capacity, *Angew. Chem., Int. Ed.*, 2017, **56**, 11426–11430.

36 J. A. Mason, M. Veenstra and J. R. Long, Evaluating metal–organic frameworks for natural gas storage, *Chem. Sci.*, 2014, **5**, 32–51.

37 D. A. Gómez-Gualdrón, T. C. Wang, P. García-Holley, R. M. Sawelewa, E. Argueta, R. Q. Snurr, J. T. Hupp, T. Yildirim and O. K. Farha, Understanding Volumetric and Gravimetric Hydrogen Adsorption Trade-off in Metal–Organic Frameworks, *ACS Appl. Mater. Interfaces*, 2017, **9**, 33419–33428.

38 C. Song, H. Liu, J. Jiao, D. Bai, W. Zhou, T. Yildirim and Y. He, High methane storage and working capacities in a NbO-type metal–organic framework, *Dalton Trans.*, 2016, **45**, 7559–7562.

39 Y. He, F. Chen, B. Li, G. Qian, W. Zhou and B. Chen, Porous metal–organic frameworks for fuel storage, *Coord. Chem. Rev.*, 2018, **373**, 167–198.

40 T. N. Tu, H. T. D. Nguyen and N. T. Tran, Tailoring the pore size and shape of the one-dimensional channels in iron-based MOFs for enhancing the methane storage capacity, *Inorg. Chem. Front.*, 2019, **6**, 2441–2447.

41 H. Furukawa, N. Ko, Y. B. Go, N. Aratani, S. B. Choi, E. Choi, A. Ö. Yazaydin, R. Q. Snurr, M. O'Keeffe, J. Kim and O. M. Yaghi, Ultrahigh Porosity in Metal-Organic Frameworks, *Science*, 2010, **329**, 424–428.

42 P. Huang, C. Chen, Z. Hong, J. Pang, M. Wu, F. Jiang and M. Hong, Azobenzene Decorated NbO-Type Metal–Organic Framework for High-Capacity Storage of Energy Gases, *Inorg. Chem.*, 2019, **58**, 11983–11987.

43 M. Krüger, A. K. Inge, H. Reinsch, Y.-H. Li, M. Wahiduzzaman, C.-H. Lin, S.-L. Wang, G. Maurin and N. Stock, Polymorphous Al-MOFs Based on V-Shaped Linker Molecules: Synthesis, Properties, and in Situ Investigation of Their Crystallization, *Inorg. Chem.*, 2017, **56**, 5851–5862.

44 L. Li, S. Wang, T. Chen, Z. Sun, J. Luo and M. Hong, Solvent-Dependent Formation of Cd(II) Coordination Polymers Based on a C2-Symmetric Tricarboxylate Linker, *Cryst. Growth Des.*, 2012, **12**, 4109–4115.

45 A. Schoedel, M. Li, D. Li, M. O'Keeffe and O. M. Yaghi, Structures of Metal–Organic Frameworks with Rod Secondary Building Units, *Chem. Rev.*, 2016, **116**, 12466–12535.

46 V. Colombo, S. Galli, H. J. Choi, G. D. Han, A. Maspero, G. Palmisano, N. Masciocchi and J. R. Long, High thermal and chemical stability in pyrazolate-bridged metal–organic frameworks with exposed metal sites, *Chem. Sci.*, 2011, **2**, 1311–1319.

47 Y.-F. Zhang, Z.-H. Zhang, L. Ritter, H. Fang, Q. Wang, B. Space, Y.-B. Zhang, D.-X. Xue and J. Bai, New Reticular Chemistry of the Rod Secondary Building Unit: Synthesis, Structure, and Natural Gas Storage of a Series of Three-Way Rod Amide-Functionalized Metal–Organic Frameworks, *J. Am. Chem. Soc.*, 2021, **143**, 12202–12211.

48 Y.-L. Zhao, Q. Chen, J. Lv, M.-M. Xu, X. Zhang and J.-R. Li, Specific sensing of antibiotics with metal-organic frameworks based dual sensor system, *Nano Res.*, 2022, **15**, 6430–6437.

49 A. Spek, Single-crystal structure validation with the program PLATON, *J. Appl. Crystallogr.*, 2003, **36**, 7–13.

50 F. Gándara, H. Furukawa, S. Lee and O. M. Yaghi, High Methane Storage Capacity in Aluminum Metal–Organic Frameworks, *J. Am. Chem. Soc.*, 2014, **136**, 5271–5274.

51 Y. Peng, V. Krungleviciute, I. Eryazici, J. T. Hupp, O. K. Farha and T. Yildirim, Methane Storage in Metal–Organic Frameworks: Current Records, Surprise Findings, and Challenges, *J. Am. Chem. Soc.*, 2013, **135**, 11887–11894.

52 X. Duan, C. Wu, S. Xiang, W. Zhou, T. Yildirim, Y. Cui, Y. Yang, B. Chen and G. Qian, Novel Microporous Metal–Organic Framework Exhibiting High Acetylene and Methane Storage Capacities, *Inorg. Chem.*, 2015, **54**, 4377–4381.

53 Y. He, W. Zhou, T. Yildirim and B. Chen, A series of metal–organic frameworks with high methane uptake and an empirical equation for predicting methane storage capacity, *Energy Environ. Sci.*, 2013, **6**, 2735–2744.

54 T. Takei, J. Kawashima, T. Ii, A. Maeda, M. Hasegawa, T. Kitagawa, T. Ohmura, M. Ichikawa, M. Hosoe, I. Kanoya and W. Mori, Hydrogen Adsorption Properties of Lantern-Type Dinuclear M(BDC)(DABCO)$_{1/2}$, *Bull. Chem. Soc. Jpn.*, 2008, **81**, 847–856.

6532 | *Inorg. Chem. Front.*, 2022, **9**, 6527–6533

This journal is © the Partner Organisations 2022

55 Q.-R. Fang, G.-S. Zhu, Z. Jin, Y.-Y. Ji, J.-W. Ye, M. Xue, H. Yang, Y. Wang and S.-L. Qiu, Mesoporous Metal–Organic Framework with Rare etb Topology for Hydrogen Storage and Dye Assembly, *Angew. Chem., Int. Ed.*, 2007, **46**, 6638–6642.

56 K. Sumida, C. M. Brown, Z. R. Herm, S. Chavan, S. Bordiga and J. R. Long, Hydrogen storage properties and neutron scattering studies of Mg$_2$(dobdc)—a metal–organic framework with open Mg^{2+} adsorption sites, *Chem. Commun.*, 2011, **47**, 1157–1159.

57 X. Liu, M. Oh and M. S. Lah, Size- and Shape-Selective Isostructural Microporous Metal–Organic Frameworks with Different Effective Aperture Sizes, *Inorg. Chem.*, 2011, **50**, 5044–5053.

58 Z. Chen, P. Li, R. Anderson, X. Wang, X. Zhang, L. Robison, L. R. Redfern, S. Moribe, T. Islamoglu, D. A. Gómez-Gualdrón, T. Yildirim, J. F. Stoddart and O. K. Farha, Balancing volumetric and gravimetric uptake in highly porous materials for clean energy, *Science*, 2020, **368**, 297–303.

This journal is © the Partner Organisations 2022

Inorg. Chem. Front., 2022, **9**, 6527–6533 | **6533**